Allosteric Communication in the Tryptophan Synthase Bienzyme Complex: Roles of the β-Subunit Aspartate 305−Arginine 141 Salt Bridge

Davide Ferrari,[‡,§] Dimitri Niks,[§] Li-Hong Yang,[⊥] Edith W. Miles,[||] and Michael F. Dunn*[,§]

Department of Biochemistry, University of California at Riverside, Riverside, California 92521, and The National Institutes of Health, Laboratory of Biochemistry and Genetics, NIDDK, NIH, Building 8/Room 2A09, Bethesda, Maryland 20892-0830

Received February 21, 2003; Revised Manuscript Received May 1, 2003

ABSTRACT: The allosteric interactions that regulate substrate channeling and catalysis in the tryptophan synthase bienzyme complex from *Salmonella typhimurium* are triggered by covalent reactions at the β-site and binding of substrate/product to the α-site. The transmission of these allosteric signals between the α- and β-catalytic sites is modulated by an ensemble of weak bonding interactions consisting of salt bridges, hydrogen bonds, and van der Waals contacts that switch the subunits between open and closed conformations. Previous work has identified a scaffolding of salt-bridges extending between the α- and β-sites consisting of αAsp 56, βLys 167, and βAsp 305. This work investigates the involvement of yet another salt bridging interaction involving the βAsp 305−βArg 141 pair via comparison of the spectroscopic, catalytic, and allosteric properties of the βD305A and βR141A mutants with the behavior of the wild-type enzyme. These mutations were found to give bienzyme complexes with impaired allosteric communication. The βD305A mutant also exhibits altered β-site substrate reaction specificity, while the catalytic activity of the βR141A mutant exhibits impaired β-site catalytic activity. The >25-fold activation of the α-site by α-aminoacrylate Schiff base formation at the β-site found in the Na^+ form of the wild-type enzyme is abolished in the Na^+ forms of both mutants. Replacing Na^+ by NH_4^+ or Cs^+ restores the βD305A to a wild-type-like behavior, whereas only partial restoration is achieved with the βR141A mutant. These studies establish that the βD305−βR141 salt bridge plays a crucial role both in the formation of the closed conformation of the β-site and in the transmission of allosteric signals between the α- and β-sites that switch the α-site on and off.

In the tryptophan synthase $\alpha_2\beta_2$ bienzyme complex (*1*), indole, generated by the cleavage of IGP,[1] is directly transferred from the α-site to the β-site via a 25 Å long interconnecting tunnel (*2*). To ensure the efficiency of indole channeling, site−site communication in this system functions both to coordinate the catalytic activities of the α- and β-sites (Scheme 1), and to prevent the escape of indole (*2*−*16*). The allosteric transitions among conformation states play two important functions in the regulation of substrate channeling in tryptophan synthase: (a) open subunit conformation states that accommodate substrate binding and release are switched to closed conformation states that activate the sites, and (b) the conversion of the αβ-dimeric units to the closed conformation state prevents the escape of indole (*2*, *4*−*6*, *15*).

During the interconversion between open and closed conformations, an extensive set of hydrogen bonds, salt

* Corresponding author: Michael F. Dunn, Department of Biochemistry, University of California at Riverside, Riverside, CA 92521. Phone: 909-787-4235. Fax: 909-787-4434. E-mail: michael.dunn@ucr.edu.

§ University of California at Riverside.

|| The National Institutes of Health.

‡ Present address: Dipartimento di Biochimica e Biologia Molecolare, Università di Parma, 43100 Parma, Italy.

⊥ Present address: Laboratory of Biomedical Sciences; North-Shore-LIJ Research Institute; 350 Community Dr.; Manhasset, NY 11030.

[1] Abbreviations: $\alpha_2\beta_2$, native form of tryptophan synthase from *Salmonella typhimurium;* α, the alpha subunit; β, the beta subunit; L-Asp or Asp, L-aspartate; L-Arg or Arg, L-arginine; L-Ala or Ala, L-alanine; βD305A, the mutant in which Asp 305 of the beta subunit has been replaced by Ala; βR141A, the mutant in which Arg 141 of the beta subunit has been replaced by alanine; E(Ain), the internal aldimine (Schiff base); $E(Aex_1)$, aldimine intermediates formed between the PLP cofactor and L-Ser; E(GD), gem diamine species; E(A−A), the α-aminoacrylate Schiff base; $E(Q_3)$, the quinonoid intermediate that accumulates during the reaction between E(A−A) and indole; $E(Q)_{Indoline}$, the quinonoid derived from the reaction of indoline with E(A−A); $E(Aex_2)$, the L-Trp external aldimine; PLP, pyridoxal phosphate; L-Ser, L-serine; L-Trp, L-tryptophan; DIT, dihydroiso-L-tryptophan; IGP, 3-indole-D-glycerol 3′-phosphate; GP, α-glycerol-phosphate; G3P, glyceraldehyde-3-phosphate; TEA, triethanolamine; TIM, triose phosphate isomerase; GAPDH, glyceraldehyde-3-phosphate dehydrogenase; DTT, D,L-dithiothreitol; NAD, β-nicotinamide adenine dinucleotide; NADH, reduced β-nicotinamide adenine dinucleotide; BZI, benzimidazole; RSSF, rapid-scanning stopped-flow; $1/\tau_n$, apparent first-order rate constant of the *n*th relaxation; A_n, amplitude of the *n*th relaxation. MVCs, monovalent cations; PDB, protein data bank.

10.1021/bi034291a CCC: $25.00
Published on Web 06/06/2003

Scheme 1: Key Steps in the α- and β-Reactions Catalyzed by Tryptophan Synthase[a]

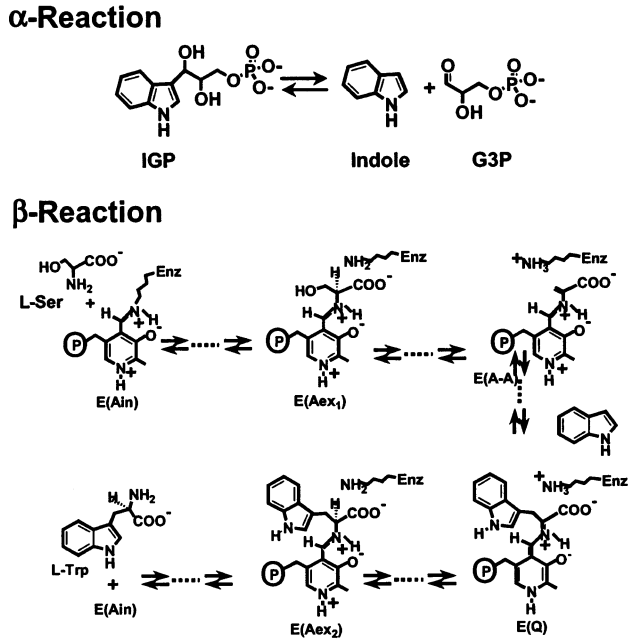

[a] The α-reaction consists of the cleavage of 3-indole-D-glycerol-3′-phosphate (IGP) to give indole and D-glyceraldehyde-3-phosphate (G3P). The β-reaction occurs in two stages. In stage I, L-Ser reacts with bound PLP of the internal aldimine, E(Ain), giving the L-Ser external aldimine, $E(Aex_1)$, which is then converted to the quasi-stable α-aminoacrylate Schiff base, E(A−A). In stage II, the indole produced at the α-site reacts with the E(A−A) at the β-site to give the quinonoid, E(Q), and L-Trp external aldimine, $E(Aex_2)$, intermediates and finally L-Trp with regeneration of E(Ain).

bridges, and van der Waals contacts that function in the regulation of substrate channeling are altered (Figure 1) (*17*−*20*). In Figure 1A, the α-subunit has the open conformation and αAsp 56 and βLys 167 are too far apart (4.10 Å) to form a salt bridge. When the α-subunit switches to the closed conformation (Figure 1B), loops 2 and 6 of the α-subunit close down over the active site, screening the site from solution (*5*, *6*, *18*). Formation of the hydrogen bonded salt bridge between αD56 and βK167 (2.79 Å) is important for this conformation change (Figure 1A,B). Since loop 2 is part of the α−β-subunit interface, this conformational change also perturbs the β-subunit (*6*, *19*). When the β-subunit switches from the open conformation (Figure 1C) to the closed conformation (Figure 1D), the two major domains that make up the β-subunit rotate relative to each other, closing the entrance to the β-active site (*10*−*12*, *18*, *19*). Formation of the hydrogen bonded salt bridge between βD305 and βR141 (2.88 Å) (Figure 1D) is important for this conformation change. These domain rotations also alter the α−β-subunit interface (*18*−*21*). The βK167−βD305 salt bridge, which has only been seen in one crystal structure (PDB file 1BKS), seems to be less important for the regulation of channeling (*12*). A set of hydrogen bonding interactions involving side chain and backbone residues also appear critically important to site−site communication in tryptophan synthase. For example, the hydrogen bond between the backbone amide N−H of αGly 181 and the carbonyl oxygen of βSer 178 is essential for the transmission of allosteric signaling between the α- and β-sites (*22*, *23*). The side chain hydroxyl of αThr 183 plays an essential role in the conformational transition between open and closed conformations of the α-subunit and plays an important role in the activation of the α-site (*18*, *21*, *24*, *25*). Another important component of this scaffolding is the monovalent cation (MVC) binding site located about 8 Å from the β-catalytic site (the $Na^+/K^+/Cs^+$ site) (*9*−*12*, *16*, *17*, *26*−*28*). This site together with the set of alternating salt-bridges formed between αD56 and βK167, βK167 and βD305, and βD305 and βR141 participate in the transmission of allosteric signals between the sites (*10*−*12*, *16*−*19*, *27*−*30*).

The side chains of βR141 and βD305 undergo relatively large displacements as the β-subunit switches between open and closed conformations (Figure 1C,D) (*13*, *17*, *18*, *20*−*23*, *31*, *32*). In those structures classified as open conformations of the β-subunit (*12*), the distance between the carboxylate of βAsp 305 and the guanidinium group of the βArg 141 side chain ranges from 5.3 to 13.2 Å (Figure 1C). In structures with open β-subunit conformations (*17*, *18*, *31*, *32*), both the carboxylate of βD305 and the guanidinium group of βR141 are usually solvent exposed. In the open conformation of the Na^+ complex of E(Ain) (*31*), the βD305 carboxylate takes up two conformations, one solvent exposed, the other involves a salt bridge with βK167 (PDB file 1BKS). In all of the closed conformations of the β-subunit (*12*, *18*), the βAsp 305−βArg 141 distances range from 2.76 to 3.13 Å, and correspond to hydrogen bonded salt-bridging charge−charge interactions (Figure 1D). The strong correlation between the formation of the βAsp 305−βArg 141 salt-bridge and the conversion to a closed β-subunit conformation supports the argument that this salt-bridge is a structural and functional signature of the closed state.

The βK87T $E(Aex_1)$ structures with either IPP or GP bound to the α-site show a conformation where the carboxylate of βD305 forms a salt bridge with βR141 and the αβ-subunit pairs exhibit closed conformations (*18*) (PDB files 2TRS and 2TRY). In the structure of the $E(Aex_1)$ form of the βK87T mutant lacking an α-site ligand, the carboxylate of βD305 makes a hydrogen bond to the side chain hydroxyl oxygen of the L-Ser Schiff base (*18*) (PDB file 1UBS). The structures of the wild-type and αT183V mutant L-Ser external aldimines (*21*) (PDB files 1KFJ and 1KFE) show that the hydroxyl group is hydrogen bonded both to the carboxylate of βAsp 305 and to the amide N−H of βAla 112. In all three structures, the α-site is unoccupied and has the open conformation, while the β-site appears closed. The hydrogen bonding of βAsp 305 to the $E(Aex_1)$ hydroxyl is fully consistent with the proposed role for βAsp 305 in substrate specificity and catalysis in the β-reaction (*16*).

In addition to the physiologically important reactions depicted in Scheme 1, tryptophan synthase also catalyzes a variety of nonphysiological reactions that have proven to be useful as probes both of the wild-type enzyme catalytic mechanism (*1*, *4*, *7*, *29*, *33*) and of the allosteric properties of metal-substituted wild-type and mutant enzymes (*2*, *4*−*6*, *9*−*12*, *16*). Two of these reactions have been used in this study to compare the catalytic and allosteric properties of the wild-type enzyme with the

βD305A and βR141A mutants. One of these reactions involves the conversion of L-Ser to ammonium ion and pyruvate (eq 1):

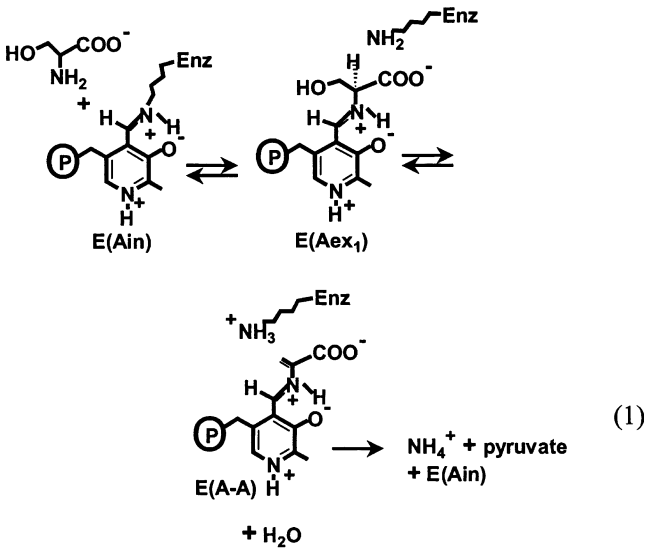

(1)

The other involves reaction of nucleophilic analogues of indole with the α-aminoacrylate intermediate to give the species E(Q) shown in eq 2:

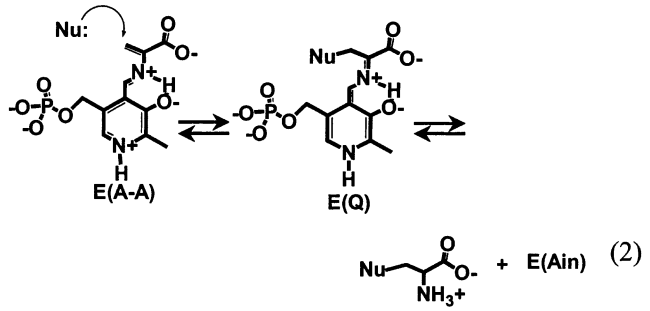

(2)

where Nu = indole, indoline, aniline, *N*-methylhydroxylamine, or methoxylamine.

As will be shown, careful comparison of the behaviors of the βD305A, βR141A, and wild-type enzymes in these reactions and in the physiologically important α-, β-, and αβ-reactions (Scheme 1), via steady-state kinetics, rapid kinetics of partial reactions, and static UV/Vis spectroscopy establishes that the salt bridge between βD305 and βR141 plays important roles both in stabilization of the closed conformation of the β-subunit, and in allosteric communication between the α- and β-sites.

MATERIALS AND METHODS

Materials. L-Ser, BZI, indole, GP, TIM, GAPDH, DTT, NAD, and D-fructose-1,6-diphosphate tetra(cyclohexylammonium) salt were purchased from Sigma. Aldolase was purchased from Worthington. Methoxylamine, *N*-methylhydroxylamine, indoline, arsenic(V) oxide hydrate, and triethanolamine were purchased from Aldrich. Aniline was purchased from Mallinckrodt. Indoline was purified by vacuum distillation and converted to its hydrochloride salt as previously described (*9*). IGP was synthesized as previously described (*34*) and by a modification involving purification of the crude IGP on a P2 Biogel column (90 × 1.5 cm). The tetra(cyclohexylammonium) salt of D-fructose-1,6-diphosphate was used to ensure that pure IGP was sodium ion free. A more detailed description of this purification will be presented elsewhere. The βR141A mutant was prepared using the expression vector pEBA-10 as the template for quick and convenient mutagenesis by megaprimer PCR (*35*). The mutagenic primer, GG CGA CTG GGC CTC AAC GTC, and the primer PE6 (*35*) (which contains an *Sph* I restriction site) were used to amplify the first round of PCR with the pEBA-10 template plasmid using Pfu DNA polymerase. The first round PCR fragments were purified and used directly as primers together with the alternate primer PE7 (which contains a *Bgl* II restriction site) to amplify a second round of DNA synthesis. The second round PCR fragments were purified and blunt-end inserted into the linearized pGEM-5zf(+) vector (Promega). The linearized pGEM-5zf(+) was prepared by digestion with EcoRV to produce blunt-ends and was dephosphorylated with alkaline phosphatase to suppress self-ligation and circularization. After confirmation of the mutation by DNA sequencing, the inserted DNA fragment was liberated with *Bgl* II and *Sph* I and ligated into the original parent plasmid (pEBA-10) which had also been digested with *Bgl* II and *Sph* I. Growth of the *Escherichia coli* host strain CB149 harboring the wild type or the R141A mutant form of plasmid EBA-10 that expresses the wild type or the R141A mutant form of the *Salmonella typhimurium* tryptophan synthase $\alpha_2\beta_2$ complex and purification of the wild type or mutant $\alpha_2\beta_2$ complex were performed as previously described (*10*, *12*, *28*, *34*−*38*).

UV/Visible Absorbance Measurements. Static UV/Vis absorbance spectra and activity measurements were performed on a Hewlett-Packard 8452A diode array spectrophotometer at 25 ± 2 °C in 50 mM pH 7.8 TEA buffer. To measure the activity of the α-, β-, and αβ-reactions, the absorbance at 290 nm was recorded after mixing the enzyme with the appropriate substrates and effectors. The α-reaction was followed measuring the decrease in absorbance due to the cleavage of IGP to indole and G3P ($\Delta\epsilon = -1.39$ mM^{-1} cm^{-1}) (*39*). The β-reaction was followed measuring the increase in absorbance due to the conversion of indole to L-Trp ($\Delta\epsilon = 1.89$ mM^{-1} cm^{-1}) (*10*, *38*). The overall αβ-reaction was followed measuring the increase in absorbance due to the conversion of IGP to L-Trp ($\Delta\epsilon = 0.56$ mM^{-1} cm^{-1}) (*10*, *39*) or in a coupled enzyme assay using glyceraldehyde-3-phosphate dehydrogenase (GAPDH), NAD, and arsenate ion (*40*). For the coupled assay, solutions were supplemented with a 50 mM arsenate-TEA buffer, pH 7.8, containing 0.5 mM NAD, 2 mM D,L-dithiothreitol (DTT), and excess GAPDH. The use of this arsenate buffer (this buffer was specifically chosen to keep coupling solutions MVC-free) results in coupling rates that are reduced relative to the sodium arsenate/tetrasodium pyrophosphate buffer system recommended by Worthington (*40*). Thus, coupling rates in Table 1 were modified by a factor of 1.163 to account for this discrepancy. The nature of the discrepancy probably has its origins in the excess TEA (~400 mM) added to adjust the pH of the arsenate buffer to 7.8. Coupling reactions were monitored at 338 nm, the absorption maximum of NADH ($\epsilon = 6.22$ mM^{-1} cm^{-1}). The coupled assay was used

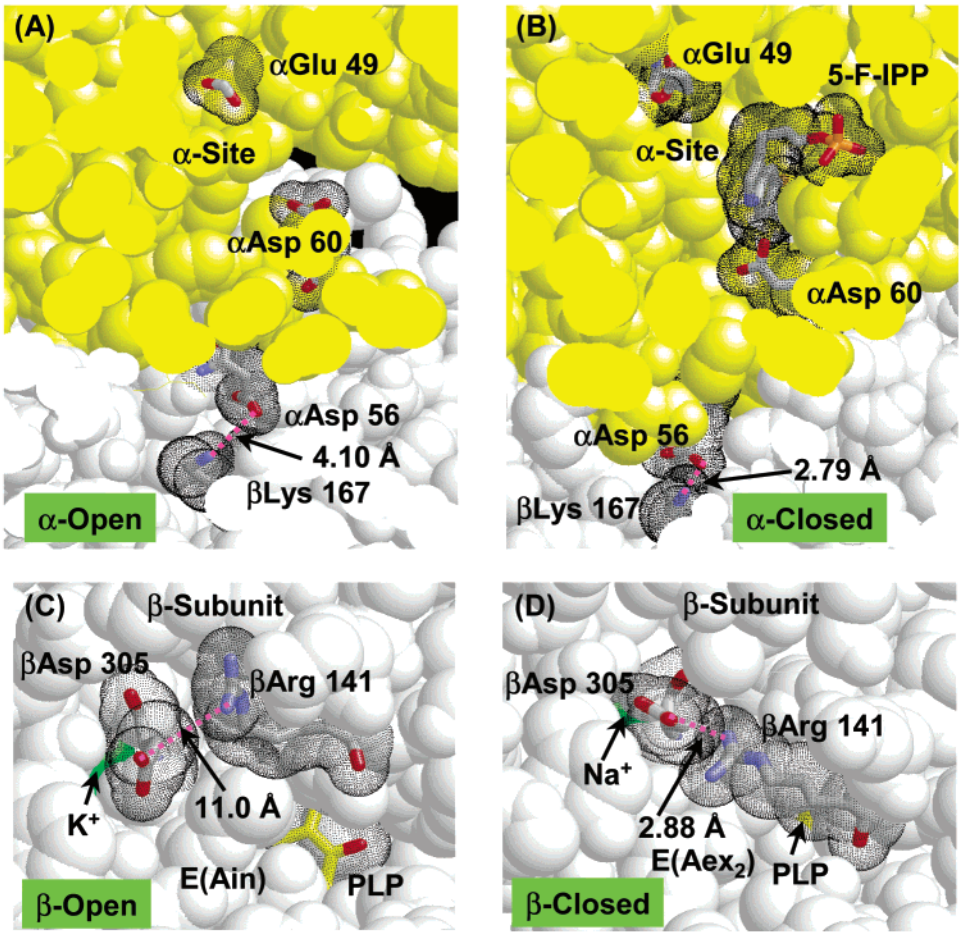

FIGURE 1: Structural details for the αAsp 56−*β*Lys 167 and *β*Asp 305−*β*Arg 141 pairs in the internal aldimine, E(Ain), (A, C) the α-site complex with 5-fluoro-IGP (B), and the L-Ser external aldimine, E(Aex$_2$), formed with the *β*K87T mutant, (D). The α-subunits are shown in yellow and the *β*-subunits in monochrome. The E(Ain) structure (A) and (C) has the open conformation for both the α- and *β*-subunits, while the 5-fluoro IGP complex (B) has the closed α-subunit conformation, and the mutant E(Aex$_2$) structure (D) has the closed *β*-subunit conformation. In (A) and (B), some residues have been cut away to show the catalytic site residues αGlu 49 and αAsp 60 and the αAsp 56−*β*Lys 167 pair (stick representation in CPK colors with the van der Waals surfaces in black dots). In (B), 5-fluoro-IGP is also shown in stick representation with a dotted van der Waals surface. The structures in (C) and (D) show the pyridoxal phosphate (PLP) ring system in yellow/red sticks and the *β*Arg 141−*β*Asp 305 pair shown in CPK colored sticks (all with van der Waals surfaces in black dots). The monovalent cation (green) in each structure (K^+ or Na^+) is almost completely buried. In panel (D), *β*Lys 167 is faintly visible as a wireframe representation so that the *β*Asp 305−*β*Arg 141 interaction is not obscured. In panels (A−D), distances are shown as magenta dotted lines. In the closed structures of the 5-fluoro-IGP complex (B) and the E(Aex$_2$) intermediate (D), the pairs αAsp 56−*β*Lys 167 and *β*Asp 305−*β*Arg 141 form hydrogen bonded salt bridges, while in the open structures of E(Ain) (A) and (C), these pairs are too far apart to form hydrogen bonded salt bridges. The structures are rendered from PDB file 1TTQ (A) and (C) (*18*), PDB file 1A50 (B) (*20*), and PDB file 2TSY (D) (*18*).

to ensure that pyruvate formation did not significantly interfere with the measurement of the α*β*-reaction and to provide a direct estimate of the α-activity of *β*R141A under these conditions.

The *β*-activity for the reactions of *β*R141A with the indole substrate analogue indoline was measured by following the absorbance change at 302 nm using $\Delta\epsilon = 1.5\ mM^{-1}\ cm^{-1}$ (*16*). The contribution due to the formation of pyruvate was calculated by following the absorbance time courses at both 320 and 350 nm where only pyruvate contributes to the absorption spectrum (*16*) and corrections for pyruvate formation were made as necessary.

UV/Visible Titration Studies. Titrations of the wild-type and *β*R141A mutant enzymes with L-Ser were performed to determine the apparent dissociation constants for the L-Ser reaction at 25° ± 2 °C in 50 mM pH 7.8 TEA buffer. Measurements were carried out in the presence of 5 mM benzimidazole (BZI) to inhibit the production of pyruvate (an unwanted side reaction) and also to stabilize E(A−A) as the complex with BZI (*16*). The appearance of the E(A−A) species was followed at 350 nm. Titration plots were fitted to the following equation: $A = [\text{L-Ser}](A_\infty - A_0)/(K_{Dapp} + [\text{L-Ser}])$, where A is the observed absorbance and A_∞ and A_0 are the absorbance values extrapolated to infinite and 0 [L-Ser], respectively. Since the appearance of E(A−A) involves both binding and chemical steps, the measured values give apparent dissociation constants, K_{Dapp}.

Stopped-Flow Fluorescence Measurements. Rapid kinetic measurements were performed as previously described at 25 ± 2 °C in 50 mM pH 7.8 TEA buffer (*9*−*12*, *16*). The rapid formation and decay of E(Aex$_1$) was followed by measuring the envelope of fluorescence emission (using $\lambda_{ex} = 425$ nm) provided by cutoff filters (*9*, *41*). The

Table 1: Summary Comparing the Steady-State Reaction Rates[a] for the α-, β-, and αβ-Reactions and the Activation of the α-Site by L-Ser Reaction at the β-Site[b]

	α (s^{-1})			β (s^{-1})			αβ (s^{-1})				αβ/α[d]		
							βR141A						
effectors	wt	βR141A	βD305A	wt	βR141A	βD305A	wt	direct[b]	coupled[c]	βD305A	wt	βR141A	βD305A
none	0.3	0.36	0.44	1.6	0.033	0.88	0.3	0.16		0.3	1	0.4	0.7
Na^+	0.1	0.074	0.30	7.4	0.028	0.40	3	0.066	0.057	0.04	30	0.9	0.1
K^+	0.1	0.068	0.28	11	0.037	0.80	2.6	0.099	0.080	0.28	26	0.7	1
NH_4^+	0.05	0.083	0.30	13	0.23	5.0	2	0.35	0.33	2.94	40	4	9
Cs^+	0.07	0.039	0.30	14	0.62	7.8	3.8	0.72	0.72	3.14	54	18	10
GP				0.4	0.12	0.54							
Na^+ + GP				2.9	0.087	0.56							
NH_4^+ + GP				1.4	0.55	1.56							

[a] Reaction rates are measured as v/[E] where v is the steady-state rate measured with 0.5−2 μM enzyme under the following conditions: α-reaction: [IGP] = 0.2 mM; β-reaction, [L-Ser] = 40 mM, [indole] = 0.2 mM; αβ-reaction; [IGP] = 0.2 mM, [L-Ser] = 40 mM all in 50 mM pH 7.8 TEA buffer at 25 °C. Effector concentrations: [NaCl] = 100 mM; [KCl] = 100 mM; [NH_4Cl] = 50 mM; [CsCl] = 100 mM; [GP] = 50 mM. [b] The biphasic time course is comprised of a negative phase (α-reaction) followed by a positive phase (αβ-reaction). [c] The activity of tryptophan synthase is coupled to the activity of glyceraldehyde-3-phosphate dehydrogenase as described in Materials and Methods; the activity of the coupling enzyme can be used to approximate the activity of the α-site. [d] Activation of the α-site by reaction of L-Ser at the β-site is given by the ratio of the αβ-rate (direct measurement) divided by the α-rate (αβ/α). Errors in steady-state rate measurements are estimated to be ±10%.

fluorescence time courses were fitted by nonlinear least-squares regression analysis to a sum of exponentials according to eq 3:

$$F_t = F_\infty + \Sigma_i F_i \exp(-t/\tau_i) \quad (3)$$

where F_t is the fluorescence at time t, F_∞ is the final fluorescence, F_i is the fluorescence due to the ith relaxation, and $1/\tau_i$ corresponds to the observed rate for the ith relaxation. Analysis of stopped-flow fluorescence and UV/Vis absorption time courses were performed using the software Peakfit (version 4, Jandel Scientific) and Sigmaplot (version 4, SPSS).

RESULTS

Steady-State Kinetic Activities for the Reactions Catalyzed by the Wild-Type, βR141A and βD305A Bienzyme Complexes. Steady-state activities for the α-reaction (cleavage of IGP), the β-reaction (L-Ser + indole) (Scheme 1) and the αβ-reaction (L-Ser + IGP) for the wild-type enzyme, and the βR141A and βD305A mutants are summarized in Table 1. The rates of the α-reaction are essentially unaffected by the MVCs and do not show significant differences between wild-type and mutant enzymes. Since both mutations are located in the β-subunit far away from the α-site, this result is not surprising.

In the βD305A mutant system, Na^+ and K^+ do not stimulate the β-reaction (*16*), whereas, with NH_4^+ or Cs^+, a wild type-like activity is largely recovered. In the βR141A mutant system, the β-reaction shows very low activity in the presence of Na^+, K^+, or in the absence of effectors. Only NH_4^+ and Cs^+ were found to significantly activate the β-reaction (Table 1).

The αβ-reaction catalyzed by the βD305A mutant enzyme follows the same behavior observed for the β-reaction: the binding of either NH_4^+ or Cs^+ restores a wild-type-like behavior. In the βR141A mutant, the αβ-reaction could be measured directly by observing the absorbance changes at 290 nm for the NH_4^+ and Cs^+ forms of the enzyme. Attempts to measure the αβ-reaction via the direct assay for the Na^+ and K^+ forms of the mutant or the MVC-free mutant gave

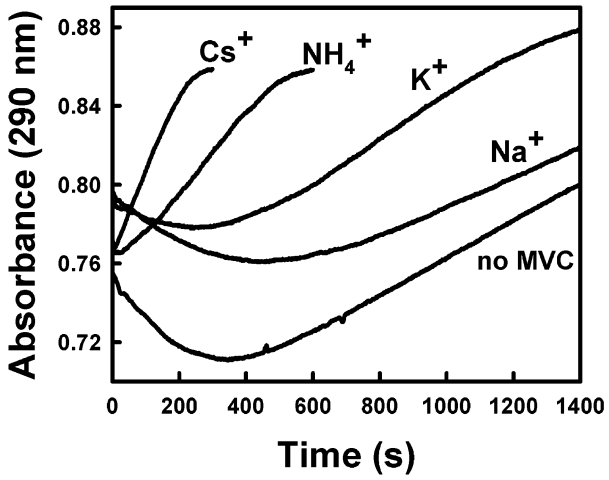

FIGURE 2: Plot of absorbance at 290 nm versus time for the αβ-reaction for the βR141A mutant. The rate data from experiments such as these are summarized in Table 1. Reaction conditions: [enzyme] = 0.5 μM ($\alpha_2\beta_2$) for the MVC-free, NH_4^+, and Cs^+ forms of the enzyme or 1 μM ($\alpha_2\beta_2$) for the Na^+ and K^+ forms of the enzyme, [IGP] = 0.2 mM, [L-Ser] = 40 mM all in 50 mM pH 7.8 TEA buffer at 25 °C. When present, effector concentrations were as follows: 100 mM Na^+, 100 mM K^+, 50 mM NH_4^+, or 100 mM Cs^+.

290 nm time courses showing an initial decrease in absorbance that is characteristic of the α-reaction (Figure 2). Then, after 3−6 min, there occurred a progressive increase in absorbance characteristic of the αβ-reaction. In contrast to this behavior, the time courses for the wild-type enzyme are essentially linear. These observations indicate that the α- and β-reactions are not tightly coupled for these forms of the mutant, and that indole escape from the bienzyme complex is a significant process. The indirect assay measures the rate of G3P production due to IGP cleavage (α-reaction) under the conditions where L-Ser is bound to the β-site. The steady-state rate for this cleavage indicates that the α-reaction is much slower than the β-reaction for all forms of the mutant. The subsequent increase in absorbance observed in the direct assay then appears due to the build up of indole in the solution as IGP is slowly cleaved. In agreement with this

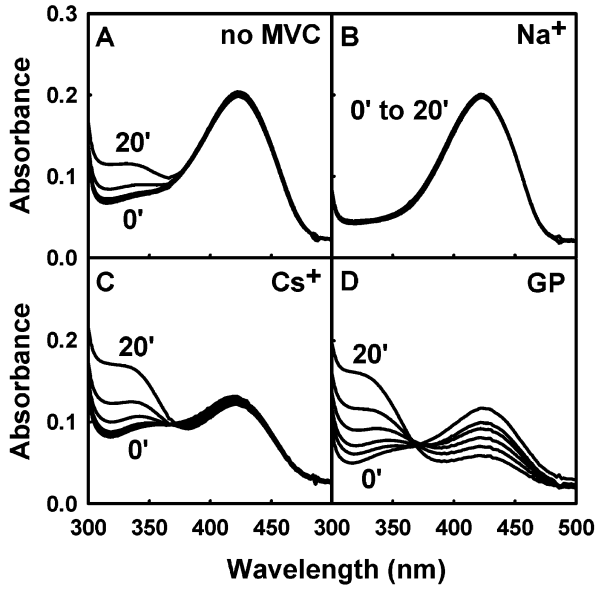

FIGURE 3: Time-resolved spectra showing the UV/Vis absorption changes resulting from the reaction of L-Ser with the MVC-free (A), Na^+- (B), Cs^+- (C), or GP-bound (D) forms of the βR141A mutant of tryptophan synthase. Spectra were recorded at various intervals between 0 and 20 m. The spectrum designated as time zero was measured about 5−10 s after mixing enzyme and L-Ser. Reaction conditions: 10 μM enzyme ($\alpha_2\beta_2$), 40 mM L-Ser, and when present, 100 mM Na^+, 100 mM Cs^+ or 50 mM GP, all in 50 mM pH 7.8 TEA buffer at 25 °C.

conclusion, addition of 0.05 mM of exogenous indole during the initial phase greatly enhanced the rate of appearance of L-Trp (data not shown).

Static UV/Visible Absorbance Measurements. (a) Reaction of L*-Ser with βR141A.* The reaction of βR141A with L-Ser results in the formation of E(Aex_1) and E(A−A). The E(A−A) intermediate then undergoes transformation to pyruvate at a significant rate (eq 1). Figure 3 summarizes the UV/Vis spectral changes that occur upon reaction of βR141A with 40 mM L-Ser at pH 7.8 for a time period of 20 min. In the absence of MVCs and α-site ligands, the production of pyruvate, as measured by the appearance of absorbance at 320 nm, is significant. However, when either Na^+ or K^+ is bound to the MVC-site, pyruvate formation is nearly completely suppressed. The binding of NH_4^+, Cs^+, or MVC-free GP stimulates pyruvate formation. The spectral changes for the GP-bound mutant show, in addition to the high rate of pyruvate production, the disappearance of the band at 424 nm characteristic of E(Ain). This spectral change is consistent with the covalent inactivation of the enzyme in a process previously described for other tryptophan synthase mutants and for aspartate aminotransferase and glutamate decarboxylase (*16*, *29*, *42*−*44*). The combination of GP and Na^+ shows spectral changes resulting from both pyruvate formation and from the covalent inactivation reaction (data not shown). These processes occur more slowly than in the presence of MVC-free GP only.

(b) Time-Resolved Spectra. The influence of MVC effectors (Na^+, NH_4^+, and Cs^+) and the α-site ligand, GP, on spectral changes observed in the reaction of L-Ser with wild-type enzyme and with the βD305A and the βR141A mutant enzymes (eq 1) and in the reaction of L-Ser and indoline (eq 4) are compared in Figures 4 and 5, respectively.

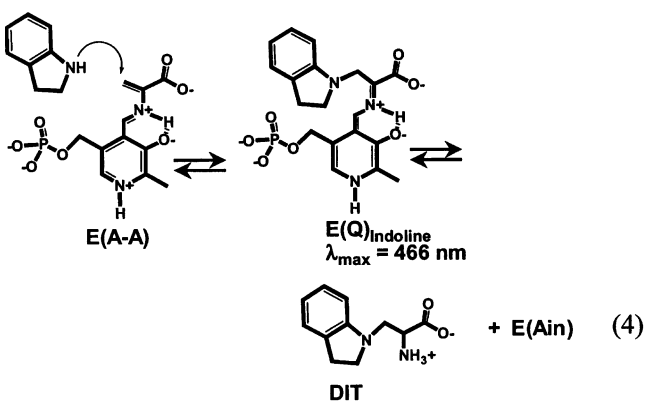

(4)

These comparisons provide information about the influence of effectors and the influence of the mutations on the stabilities of intermediates that accumulate at the β-site during these reactions. To avoid absorbance contributions arising from the formation of pyruvate and from the covalent inactivation reaction (see Figure 3), spectra were recorded within a few seconds after the addition of L-Ser.

At pH 7.8 and 25 °C, the distribution of species formed in the reaction of L-Ser with wild-type enzyme (Figure 4A) strongly favors E(A−A) (λ_{max} = 350 nm, shoulder 400−520 nm) (*9*−*12*, *41*, *45*). Of the effectors shown in Figure 4A, only Na^+ causes a significant shift in the distribution, and even so, the distribution still favors E(A−A) over E(Aex_1).

In comparison to the behavior of the wild-type enzyme, when L-Ser reacts with either the βD305A mutant or the βR141A mutant, the distribution of intermediates formed in the presence of K^+, Na^+, NH_4^+, or GP plus Na^+ favors E(Aex_1) in each instance (Figure 4B,C). In the βD305A system, the distribution of E(Aex_1) and E(A−A) formed is comparable in the presence of Cs^+, NH_4^+, GP, or GP plus Na^+, whereas the distribution is shifted strongly in favor of E(Aex_1) by Na^+ (Figure 4B). In the βR141A system, residual amounts of E(A−A) are evident in the changes at ∼350 nm for the MVC-free and NH_4^+ systems (Figure 4C). The spectra measured in the presence of Cs^+ or GP also are dominated by E(Aex_1), but show the presence of some E(A−A) (Figure 4C).

Figure 5 shows spectra for the reaction of tryptophan synthase with L-Ser and the indole analogue, indoline. In the wild-type system, this reaction gives a quasi-stable quinonoid species, $E(Q)_{Indoline}$, resulting from the nucleophilic attack of the indoline N-1 on the β-C of the E(A−A) intermediate (eq 4) (*33*). As is evident in Figure 5B,C, the accumulation of $E(Q)_{Indoline}$ is greatly impaired in the βD305A (*16*) and βR141A mutants. Trace amounts of $E(Q)_{Indoline}$ are formed with the MVC-free, NH_4^+, GP, and Na^+ plus GP forms of βD305A, while only the Cs^+ species gives a substantial amount of $E(Q)_{Indoline}$ (*16*) (Figure 5B). The accumulation of $E(Q)_{Indoline}$ is even more impaired in the βR141A mutant; only the Cs^+ complex gives a trace amount of the quinonoid species (Figure 5C). The GP complex undergoes a very slow formation of $E(Q)_{Indoline}$, with the characteristic peak at 466 nm appearing over 15−20 min following the addition of L-Ser and indoline.

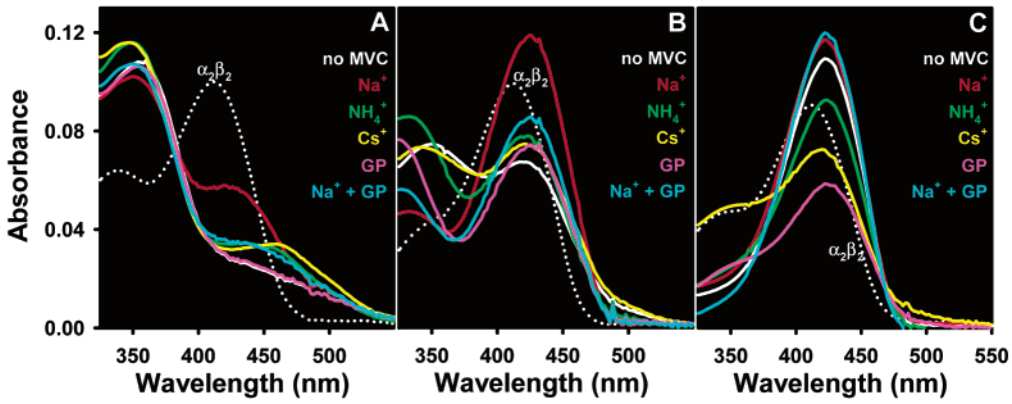

FIGURE 4: Summary of UV/Vis spectra showing the influence of allosteric effectors on the spectrum of the complex initially formed during the reaction of L-Ser with wild-type enzyme (A), the βD305A mutant (B), or the βR141A mutant (C). Spectra were measured within a few seconds after mixing so that the slow conversion of L-Ser to pyruvate (Figure 3) makes insignificant contributions to the spectra. Reaction conditions: 10 μM enzyme ($\alpha_2\beta_2$), 40 mM L-Ser, and when present, the concentrations of allosteric effectors were as follows: 100 mM Na^+, 50 mM NH_4^+, 100 mM Cs^+, and 50 mM GP, all in 50 mM pH 7.8 TEA buffer at 25 °C. The data for wild-type enzyme and for βD305A were taken from Ferrari et al. (*16*).

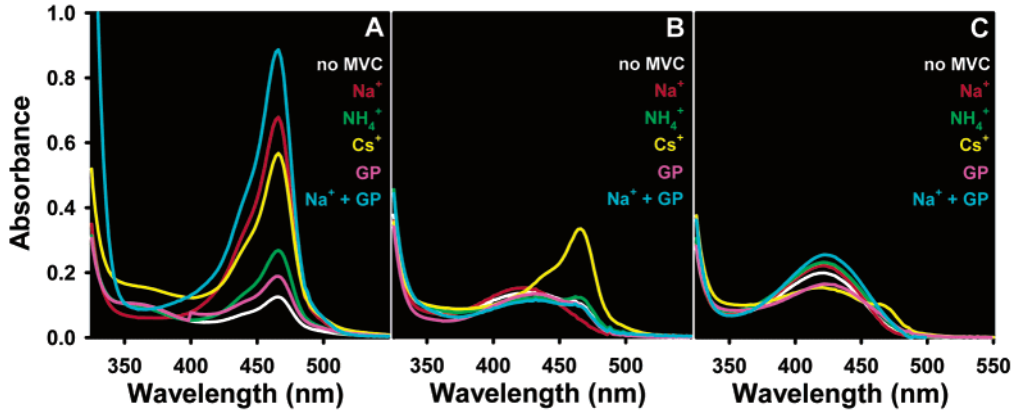

FIGURE 5: The influence of allosteric effectors on the formation of the indoline quinonoid species for wild-type enzyme (A), the βD305A mutant (B), and the βR141A mutant (C). The UV/Vis absorbance spectra were measured a few seconds after mixing 40 mM L-Ser and 5 mM indoline with enzyme. When present, the concentrations of allosteric effectors were as follows: 100 mM Na^+, 50 mM NH_4^+, 100 mM Cs^+, and 50 mM GP, all in 50 mM pH 7.8 TEA buffer at 25 °C. The data for wild-type enzyme and the βD305A were taken from Ferrari et al. (*16*).

(c) L-Ser Titration. The binding of benzimidazole (eq 5) strongly stabilizes the E(A−A) intermediate (eq 1) (*2*, *16*, *33*, *46*, *47*).

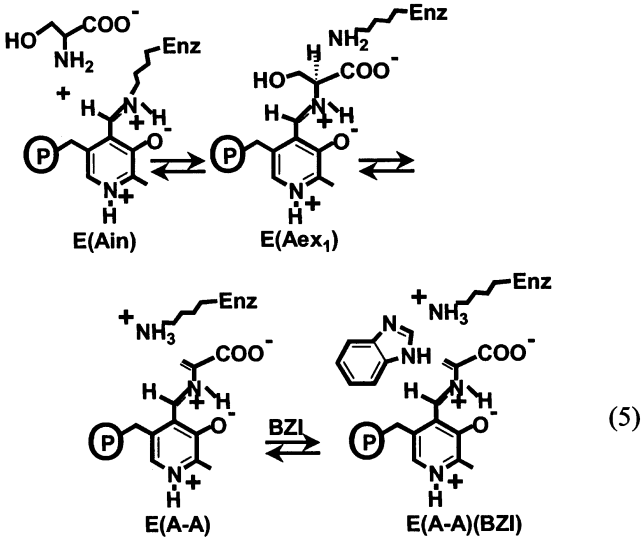

(5)

Because E(A−A) formation in the βR141A mutant system is strongly impaired (viz., Figures 4 and 6), titrations were carried out in the presence of benzimidazole so that the distribution of species is shifted in favor of E(A−A), thereby providing a spectral change common to all three systems for comparing the apparent affinities of mutant and wild-type enzymes for L-Ser. The apparent dissociation constants, K_{Dapp}, obtained in the presence of benzimidazole (Table 2) were determined by fitting the titration curves to a hyperbolic expression (Figure 6C,D) as previously described (*16*). The K_{Dapp} values calculated for wild-type and βR141A mutant enzymes in the presence of 5 mM benzimidazole were found to be very similar (Figure 6C and Table 2), whereas the K_{Dapp} value for the βD305A mutant measured under the same conditions (Figure 6D and Table 2) is more then 30-fold greater.

(d) Stopped-Flow Fluorescence Measurements. The formation of $E(Aex_1)$ involves both the L-Ser binding step and the chemical processes of $E(GD_1)$ and $E(Aex_1)$ formation, whereas the decay phase reflects the approach to equilibrium as $E(Aex_1)$ is converted to the E(A−A) species with the attendant interconversion between open and closed conformations (*4*−*6*, *10*−*13*, *15*). Comparison of these phases for mutant and wild-type enzymes (Figure 7) gives detailed information regarding the influence of the mutations on the first stage of the β-reaction (*10*−*12*, *16*).

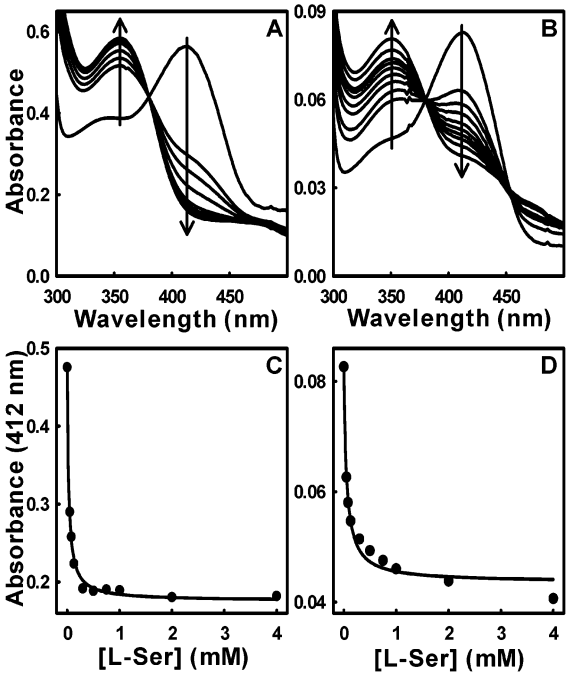

FIGURE 6: Titration of wild-type enzyme (A) and (C) and βR141A mutant (B) and (D) with L-Ser in the presence of benzimidazole (BZI). The changes in absorption spectra as a function of [L-Ser] are shown in (A) and (B), and the change in absorbance at 412 nm taken from (A) and (B) are shown in (C) and (D). The solid lines in (C) and (D) are the best fit of the data to the equation for a hyperbolic dependence of absorbance on L-Ser concentration (see text and Table 2). Reaction conditions: [enzyme] = 30 μM ($\alpha_2\beta_2$) wild-type or 10 μM ($\alpha_2\beta_2$) βR141A, [BZI] = 5 mM, [L-Ser] = 0.05, 0.08, 0.13, 0.3, 0.5, 1, 2, 4, and 7 mM (wild-type only), all in 50 mM pH 7.8 TEA buffer at 25 °C.

Table 2: Apparent Dissociation Constants, K_{Dapp}, from the Titration of Wild-Type, βR141A, or βD305A Mutant Enzymes with L-Ser in the Presence of Benzimidazole[a]

enzyme	K_{Dapp} (μM)
wild-type	23
βR141A	34
βD305A	800[b]

[a] The data were fitted to the equation: $A = [\text{L-Ser}](A_\infty - A_0)/(K_{Dapp} + [\text{L-Ser}])$, where A is the absorbance and A_∞ and A_0 are the absorbance when the [L-Ser] is ∞ and 0, respectively. Error limits are estimated to be ±10%. [b] Ferrari et al. (*16*).

The stopped-flow fluorescence time courses presented in Figure 7 compare wild-type enzyme (A) with the βR141A mutant (B) for stage I of the β-reaction. E(Aex_1) is the only species in the tryptophan synthase pathway that gives a significant fluorescence signal under these conditions. Irradiation with λ_{ex} = 425 nm and monitoring the fluorescence emission envelope provides time courses for the formation and decay of the E(Aex_1) intermediate. Table 3 summarizes the relaxation rate constants and amplitudes for the formation and decay of the E(Aex_1) species for wild-type and mutant enzymes for stage I of the β-reaction, for the overall β-reaction, and for the $\alpha\beta$-reaction. These parameters were extracted from the time courses shown in Figure 7 and others not shown here.

This comparison shows that the wild-type and βR141A mutant enzymes exhibit time courses for the formation of the E(Aex_1) species that are very similar, indicating that the Arg to Ala mutation does not significantly alter the chemistry

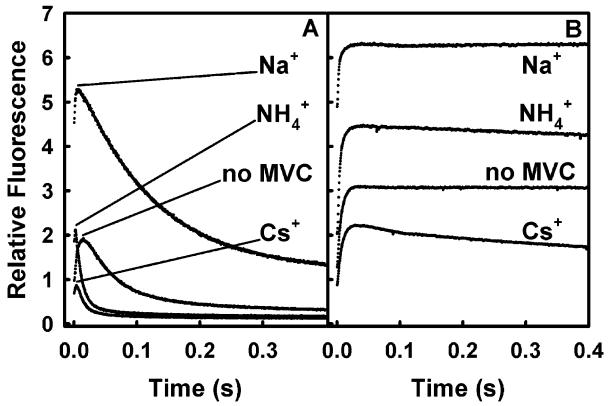

FIGURE 7: Stopped-flow kinetic time courses for wild-type enzyme (A) and βR141A mutant (B) showing the influence of monovalent cations on the formation and decay of the E(Aex_1) intermediate during stage I of the β-reaction. The reactions were carried out by mixing 80 μM enzyme sites in one syringe with 80 mM L-Ser in the other syringe. When present, the effector concentrations were as follows: 100 mM Na^+, 50 mM NH_4^+, or 100 mM Cs^+ (effector concentrations were the same in both syringes).

of this step. In contrast, the βD305A mutant in the presence of Na^+ or K^+, or in the absence of MVCs shows rates ($1/\tau_1$) for the formation of the E(Aex_1) species (Table 3) that are 3−15-fold slower than those observed for both the wild-type enzyme and the βR141A mutant. Only the presence of Cs^+ or NH_4^+ restores an almost wild-type behavior for the formation of the E(Aex_1) species (*16*).

Whereas E(Aex_1) formation is initially unaffected by the βR141A mutation, the E(Aex_1) decay time course is significantly slowed in comparison to the behavior of wild-type enzyme. The βR141A decay rates (Table 3) are 2−30 times slower (depending upon the effector present). In contrast to the wild-type and βD305A mutant enzymes, the decay phase is missing in stage I of the β-reaction in the absence of MVCs, and in the overall β-reaction both in the absence of MVCs and in the presence of NH_4^+ or Cs^+. These observations are fully consistent with the finding that the βR141A mutation provides an intrinsic stabilization of the E(Aex_1) species.

Reaction of the D305A Mutant with Indole Analogues and others Nucleophiles. (a) Benzimidazole (BZI). Previous studies (*2*, *5*, *16*, *33*) have shown that the indole analogue, benzimidazole (BZI), binds but does not covalently react with the E(A−A) species. In the wild-type system and in the βD305A mutant enzyme, BZI binds and stabilizes the E(A−A) species, giving a distribution of intermediates in stage I of the β-reaction where E(A−A) approaches 100% of the β-site species present. BZI binding also stabilizes the E(A−A) species formed with the βR141A mutant; however, under conditions where the wild-type and βD305A systems are essentially completely shifted in favor of E(A−A), the βR141A mutant gives a mixture of the E(A−A) and E(Aex_1) species in comparable amounts (Figure 6).

(b) Indoline and Aniline. Wild-type and βD305A mutant enzymes both react with L-Ser and indoline to produce the new amino acid, dihydroiso-L-tryptophan (DIT) (*16*, *21*, *33*, *48*). This reaction has been extensively studied (*2*, *5*, *16*, *33*, *48*, *49*). To determine whether the βR141A mutant exhibits altered substrate specificity, reactions with the indole analogues indoline and aniline were undertaken as previously

Table 3: Comparison of the Influence of Monovalent Cations on the Relaxations ($1/\tau$) for Formation and Decay of the E(Aex_1) Intermediate during Stage I of the β-Reaction, the Overall β-Reaction, and the $\alpha\beta$-Reaction Catalyzed by the Wild-Type Enzyme and the βD305A and βR141A Mutants[a]

	no MVCs			Na^+			NH_4^+			Cs^+		
$1/\tau$ (s^{-1})[d]	WT	βD305A	βR141A	WT	βD305A	βR141A	WT	βD305A	βR141A	WT	βD305A	βR141A
Tryptophan Synthase + L-Serine (stage I of the β-reaction)												
$1/\tau_1$ (up)	200	60	150	900	60	620	420	240	360	250	100	140
$1/\tau_2$ (up)				50−100		120			110			
$1/\tau_3$ (down)	21	1.7		7.0			90	7.6	1	70	8.0	4
Tryptophan Synthase + L-Serine + Indole (the overall β-reaction)												
$1/\tau_1$ (up)	210	46	340	900	53	540	350	250	340	200	120	125
$1/\tau_2$ (up)			120	50−100		100	120					
$1/\tau_3$ (down)	0.5						100	30		85	20	
Tryptophan Synthase + IGP (the $\alpha\beta$-reaction)												
$1/\tau_1$ (up)	250	52	200	650	64	580	480	260	360	350	120	130
$1/\tau_2$ (up)				100		100			120			
$1/\tau_3$ (down)	25	0.6		20			85	10	0.3	70	15	6

[a] Reaction conditions are the same as those described for Figure 5. [b] $1/\tau$ (up) values refer to formation of E(Aex_1) and $1/\tau$ (down) refer to decay of E(Aex_1). Error limits are estimated to be ±15%.

described (*16*). Reaction of the βR141A mutant with indoline to produce DIT was followed at 302 nm, and the time course was corrected for the absorbance changes due to pyruvate formation. The calculated activity was found to be 0.1 s^{-1}, a value identical to that of wild-type enzyme measured under the same conditions. Under these reaction conditions, aniline failed to show any of the spectral changes characteristic of the formation of a new amino acid (*16*). The time course of the reaction measured at 302 nm revealed only the progressive accumulation of pyruvate derived from the side reaction.

DISCUSSION

The spectroscopic and kinetic studies presented in this work investigate the roles played by βAsp305 and βArg141 in the kinetics, catalytic mechanism and allosteric regulation of tryptophan synthase. These studies establish the following: (a) The βAsp305 and βArg141 mutations do not substantially alter the catalytic properties of the α-subunit (Table 1). (b) However, these mutations adversely affect the β- and $\alpha\beta$-reactions, and the activation of the α-reaction by reaction of L-Ser at the β-site (Table 1). (c) The loss of α-site activation is a direct consequence of the impaired ability of the mutants to form the E(A−A) intermediate, a process coupled to formation of the closed conformation of the $\alpha\beta$-dimeric unit. (d) The monovalent cation effector, Cs^+, is particularly effective in restoring wild-type-like behavior to the βD305A mutant, but Cs^+ is much less effective in restoring the βR141A mutant (Table 1). (e) The βR141A mutation uncouples the $\alpha\beta$-reaction by impairment of the β-component of the $\alpha\beta$-reaction (Figure 2, Table 1). The βD305A mutation strongly alters substrate and reaction specificity at the β-site (*16*), whereas, the βR141A mutation has little effect on β-site specificity. The altered specificity of βD305A implies that the side chain carboxylate of βD305 plays important roles in substrate recognition and nucleophile reaction specificity. (f) The primary effect of the βR141A mutation is to alter the thermodynamics of the transition between open and closed states in favor of the open conformation. The implications of these findings are discussed in greater detail below.

Steady-State Kinetic Behavior. The βR141A and βD305A mutations do not affect the α-reaction activity (Table 1).

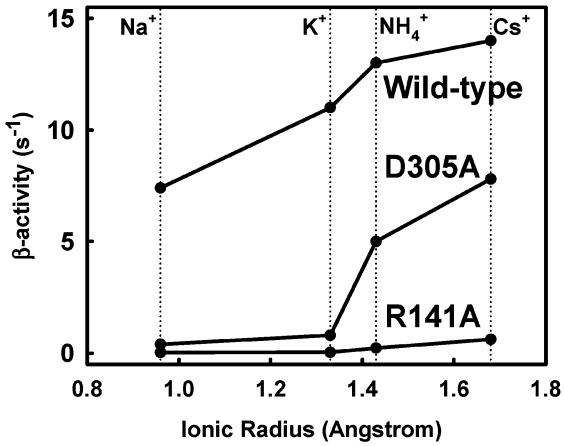

FIGURE 8: Graph showing the β-reaction activity plotted as a function of the ionic radius of the MVC effector for the wild-type enzyme, and the βD305A and βR141A mutants. Ionic radius is expressed in Angstroms. The data for wild-type enzyme and βD305A were taken from Ferrari et al. (*16*).

Nevertheless, the β-reaction, the $\alpha\beta$-reaction, and the activation of the α-reaction by E(A−A) formation all are strongly influenced by these mutations, especially in the presence of effectors (Table 1). The β- and $\alpha\beta$-activities of the two mutants measured in the presence of Na^+, K^+, NH_4^+ or without MVCs are less than the corresponding activities of wild-type enzyme by one- to more than two-orders of magnitude. The presence of Cs^+ increases the activity of βD305A ~10-fold (compared to the MVC-free mutant) and nearly restores a wild-type-like behavior. The activities of the β- and $\alpha\beta$-reactions of the βR141A mutant are significantly increased by NH_4^+ or Cs^+, but, in comparison to the wild-type enzyme, these activities are still very low (Table 1). The dependence of the β-reaction activity on the ionic radius of the MVC for each of the three enzymes (Figure 8) illustrates both the strong dependence of rate on the mutation, and the strong dependence of rate on the MVC activator bound to the β-site. Figure 8 shows a remarkable increase in rate with increasing MVC size for all three enzyme systems, suggesting that a change in radius of the MVC causes a structural perturbation that alters the microenvironment of the catalytic site, thereby altering the relative

ground state thermodynamic stabilities of covalent intermediates, and the activation energies for the interconversion of intermediates. These effects also are manifest in the dependence of intermediate distribution (Figures 4 and 5) and in the dependence of the kinetics of the formation and decay of the E(Aex$_1$) intermediate on the MVC bound to the β-site (Figure 7, Table 3). Woehl et al. (*10*, *11*), Weber-Ban et al. (*12*), and Ferrari et al. (*16*) have come to similar conclusions.

Comparison of the α- and β-reaction rates of the βR141A mutant shows that the rate of the α-reaction actually exceeds the rate of the β-reaction for the Na^+ and K^+ forms of the mutant. The low turnover rate of the strongly impaired β-site causes an uncoupling of the $\alpha\beta$-reaction in the MVC-free, Na^+, and K^+ forms of the βR141A mutant (Figure 2). As measured by the $\alpha\beta/\alpha$ rate ratio (Table 1), the reaction of L-Ser is relatively ineffective in activating the α-reaction for either mutant. Nevertheless, the NH_4^+ and Cs^+ complexes of both βD305A and βR141A give significant activation, whereas Na^+ strongly suppresses the activity of the α-site in the $\alpha\beta$-reaction of βD305A. These effects on the $\alpha\beta/\alpha$ rate ratio, together with the dependence of the fraction of sites in the form of E(A−A) on the nature of the effector bound, confirm that α-site activation by L-Ser is directly linked to the ability of the mutants both to form E(A−A) and to give closed conformations at the α- and β-sites.

Substrate Specificity Effects. Ferrari et al. (*16*) have shown that β-site substrate specificity is strongly perturbed by the βD305A mutation. The βD305A mutant exhibits greatly increased rates of pyruvate formation and synthesis of DIT from indoline and L-Ser (15-fold higher than wild-type enzyme). The βD305A mutant also catalyzes the formation of new amino acids from the reactions of aniline, *N*-methylhydroxylamine, and methoxylamine with L-Ser, whereas these nucleophilic analogues of indole rapidly react with wild-type E(A−A) to give quinonoidal species, but do not complete turnover to form new amino acids (*2*, *12*, *33*). In contrast to βD305A, the βR141A mutant exhibits a substrate specificity that is similar to the wild-type enzyme. Only the rate of pyruvate production is elevated relative to wild-type enzyme. These results strongly imply that the βD305 carboxylate has a role in substrate recognition and nucleophile reaction specificity at the β-site.

The binding and reaction of L-Ser provides another measure of substrate specificity. Benzimidazole binding strongly stabilizes E(A−A) (*2*, *16*, *33*, *47*). This interaction makes possible comparison of the relative affinities (K_{Dapp} values) of L-Ser for the E(A−A)(BZI) complexes of the wild-type, βD305A, and βR141A mutants (Table 2). The apparent dissociation constants for the wild-type and βR141A enzymes are very similar, 23 and 34 μM, respectively, whereas the βD305A mutant gives a much greater value, 800 μM. This difference in apparent affinity for L-Ser establishes that the βD305A mutation directly alters the interaction of the reacting substrate with the site, whereas the βR141A mutation does not.

The Role of Conformation Change in Tryptophan Synthase Function. Conformation change plays three well-defined roles in the tryptophan synthase system (*15*). (i) Obligatory changes in the conformation of the β-subunit function to lower activation energies for the interconversion of intermediates along the β-reaction pathway. These accommodate and facilitate the substrate motions during the bond scission/formation processes at the site (*41*, *50*). (ii) Covalent transformations at the β-site trigger the switching of the α-site between conformation states of low activity and high activity (*5*, *14*, *15*). These accomplish the coupling of the α- and β-reaction cycles in the overall $\alpha\beta$-reaction (*5*, *15*). The conversion of E(Aex$_1$) to E(A−A) is the chemical switch that activates the α-site (*5*, *11*, *12*) (Scheme 2), while conversion of E(Q$_3$) to E(Aex$_2$) is the chemical signal that reverses this activation (8). (iii) IGP and/or G3P binding to the α-site, and the conversion of E(Aex$_1$) to E(A−A) at the β-site switch $\alpha\beta$-subunit pairs to closed conformations (Figure 1, Scheme 2) that confine the indole produced by IGP cleavage to the interior compartment comprising the α- and β-sites and the interconnecting tunnel (*15*). This sequestering of indole enforces reaction with E(A−A) to form L-Trp, and thereby ensures efficiency in channeling (*2*, *5*, *12*, *15*).

The Relationship of βR141 and βD305 to the Functioning of Tryptophan Synthase. The mutation of βD305 to Ala strongly perturbs the rate of E(Aex$_1$) formation (*16*) (Table 3), a process postulated to occur via the open conformation of the β-subunit (*10*−*12*, *15*). Nevertheless, the mutation of βR141 to Ala has essentially no effect on this process (Table 3). This finding further establishes that the βD305 carboxylate plays an important role in catalysis and substrate recognition at the β-site (*16*).

Both the βD305A mutation and the βR141A mutation strongly perturb the distribution of E(Aex$_1$) and E(A−A) species formed in the L-Ser reaction (Figure 4). As we have previously shown (*9*−*12*, *16*), the interconversion of these two species is accompanied by a switch from the partially open conformation of the E(Aex$_1$) intermediate to the closed conformation of the E(A−A) intermediate (Scheme 2). Therefore, these studies establish that the destruction of the βAsp 305−βArg 141 salt-bridge via the mutation of either of these residues to L-Ala alters the thermodynamics of the conformational transition of the β-subunit to the closed state (*16*) (see Figure 4). One mechanistic consequence is the destabilization of the closed structure of the E(A−A) intermediate (Scheme 2), thus shifting the distribution of intermediates in stage I of the β-reaction in favor of E(Aex$_1$), a species with an open conformation. Hence, as shown in Figures 4 and 5, both the βR141A mutant and the βD305A mutant give distributions of intermediates that are shifted in favor of E(Aex$_1$). This effect is particularly strong for βR141A. The nearly complete reversal of the impaired catalytic activities and spectroscopic properties of the βD305A mutant by the binding of Cs^+ almost certainly has origins in the nearly complete restoration of a wild-type-like distribution of intermediates and activation energies for E(Aex$_1$) formation and decay in the β-reaction for βD305A. The partial reversal for the βR141A mutant implies that Cs^+ binding achieves only a partial restoration for βR141A.

βAsp 305, βArg 141, and the Trigger for Activation of the α-Site. This work and previous site-directed mutation studies (*12*, *16*, *23*) establish that the αAsp 56−βLys 167 and βAsp 305−βArg141 salt bridges play critically important roles in the conformational switch from open and partially open conformations to the closed conformation of the $\alpha\beta$ dimeric unit during the catalytic cycle. The structural studies of Rhee et al. (*18*) and Kulik et al. (*21*), and the solution studies of Weber-Ban et al. (*12*) and Ferrari et al. (*16*) and

Scheme 2: Cartoon Depicting the Roles of the αAsp 56−βLys 167 and βAsp 305−βArg 141 Pairs in Salt Bridging Interactions during the Catalytic Cycle of the Tryptophan Synthase Bienzyme Complex[a]

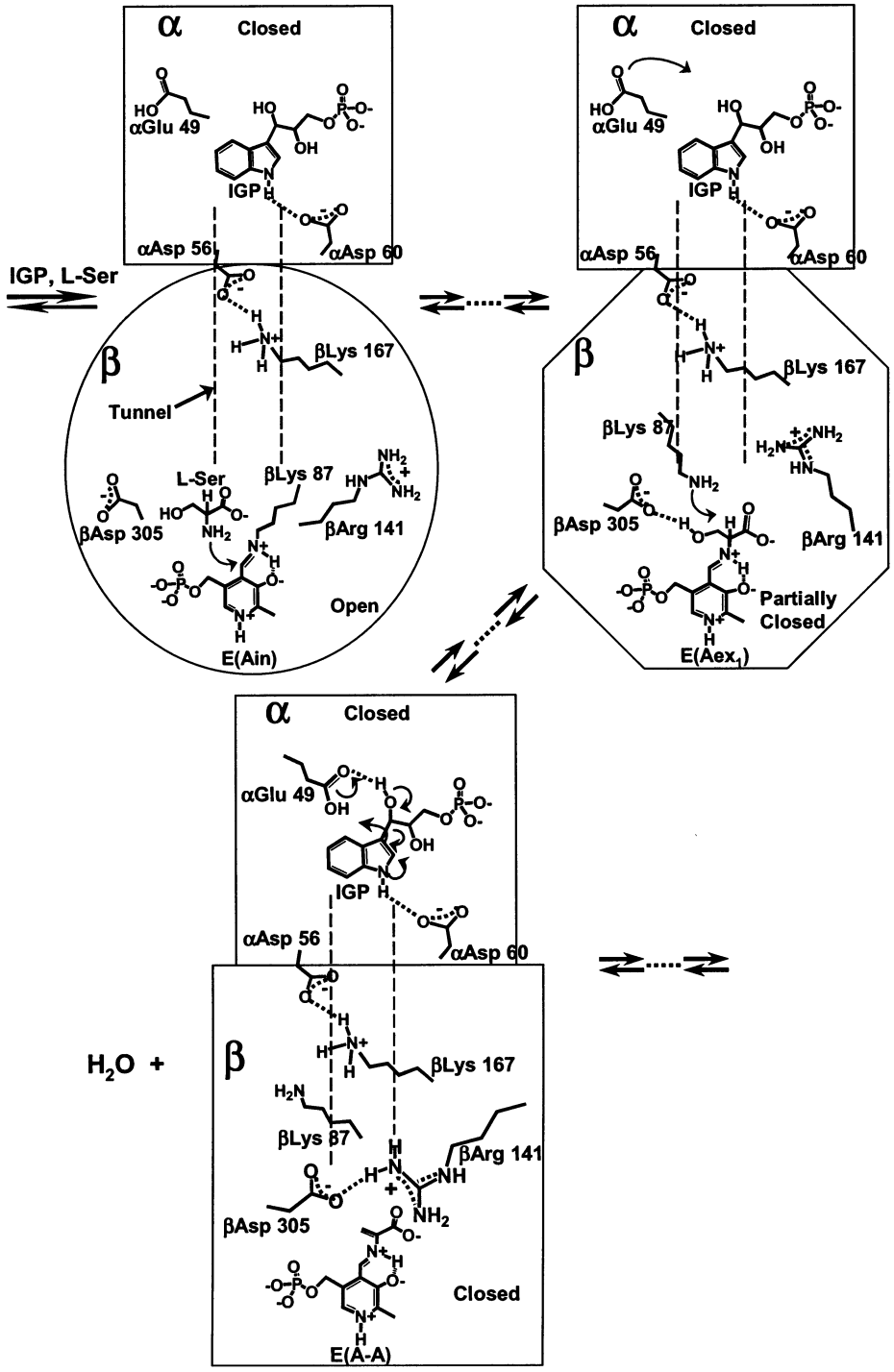

[a] β-Subunit conformations are shown as open (ellipse), partially closed (octagon), and closed (rectangle) as the β-subunit cycles from the open conformation of E(Ain) to the closed conformation of E(A−A) via the E(Aex$_1$) intermediate (the gem diamine and quinonoid species are not included in this scheme). During these transformations, the α-subunit is shown in the closed conformation (rectangle) with IGP bound. The salt-bridging status of the αAsp 56−βLys 167 and βAsp 305−βArg 141 pairs is shown at each stage together with the disposition of the catalytic groups αGlu 49 and αAsp 60 at the α-catalytic site. Activation of the α-site is shown to occur via rearrangement of the αGlu 49 side chain upon formation of the βAsp 305−βArg 141 salt-bridge and conversion of the β-subunit to the closed conformation when E(A−A) is formed.

the work presented herein reveal an additional role for βAsp 305. This role is depicted in Scheme 2. As shown in Scheme 2, when L-Ser reacts at the β-site to form the external aldimine species, the βAsp 305 carboxylate forms an hydrogen bond with the hydroxyl of this intermediate (*18*, *21*). Since mutation of βAsp 305 to Ala (*16*), but not to Asn (*12*), alters substrate specificity and impairs the rate of E(Aex$_1$) formation and decay, it is reasonable to conclude that the hydrogen bonding interaction between the βAsp 305 carboxylate and the hydroxyl of E(Aex$_1$) shown in Scheme 2 is important to the energetics of E(Aex$_1$) formation and for E(Aex$_1$) conversion to E(A−A). As reaction progresses from E(Aex$_1$) to E(A−A) (Scheme 2), the hydroxyl group is eliminated, freeing the carboxylate of βAsp 305 for salt

bridge formation with βArg 141. As depicted in Scheme 2, the resulting conformation change activates the α-site for IGP cleavage and switches the β-site to the completely closed conformation.

REFERENCES

1. Miles, E. W. (1979) *Adv. Enzymol. Relat. Areas Mol. Biol. 49*, 127−186.
2. Dunn, M. F., Aguilar, V., Brzovic, P. S., Drewe, W. F., Jr, Houben, K. F., Leja, C. A., and Roy, M. (1990) *Biochemistry 29*, 8598−8607.
3. Miles, E. W. (1991) *Adv. Enzymol. Relat. Areas Mol. Biol. 64*, 93−172.
4. Brzovic, P. S., Sawa, Y., Hyde, C. C., Miles, E. W., and Dunn, M. F. (1992) *J. Biol. Chem. 267*, 13028−13038.
5. Brzovic, P. S., Ngo, K., and Dunn, M. F. (1992) *Biochemistry 31*, 3831−3839.
6. Brzovic, P. S., Hyde, C. C., Miles, E. W., and Dunn, M. F. (1993) *Biochemistry 32*, 10404−10413.
7. Miles, E. W. (1995) in *Subcellular Biochemistry, Vol 24: Proteins: Structure, Function, and Protein Engineering* (Biswas, B. B., and Roy, S., Eds.), pp 207−254. Plenum Press, New York.
8. Leja, C. A., Woehl, E. U., and Dunn, M. F. (1995) *Biochemistry 34*, 6552−6561.
9. Woehl, E. U., and Dunn, M. F. (1995) *Biochemistry 34*, 9466−9476.
10. Woehl, E. U., and Dunn, M. F. (1999) *Biochemistry 38*, 7118−7130.
11. Woehl, E. U., and Dunn, M. F. (1999) *Biochemistry 38*, 7131−7141.
12. Weber-Ban, E. U., Hur, O., Bagwell, C., Banik, U., Yang, L.-H., Miles, E. W., and Dunn, M. F. (2001) *Biochemistry 40*, 3497−3511.
13. Miles, E. W., Rhee, S., and Davies, D. R. (1999) *J. Biol. Chem. 274*, 12193−12196.
14. Pan, P., and Dunn, M. F. (1996) *Biochemistry 35*, 5002−5013.
15. Pan, P., Woehl, E., and Dunn, M. F. (1997) *Trends Biochem. Sci. 22*, 22−27.
16. Ferrari, D., Yang, L.-H., Miles, E. W., and Dunn, M. F. (2001) *Biochemistry 40*, 7421−7432.
17. Rhee, S., Parris, K. D., Ahmed, S. A., Miles, E. W., and Davies, D. R. (1996) *Biochemistry 35*, 4211−4221.
18. Rhee, S., Parris, K. D., Hyde, C. C., Ahmed, S. A., Miles, E. W., and Davies, D. R. (1997) *Biochemistry 36*, 7664−7680.
19. Bahar, I., and Jernigan, R. L. (1999) *Biochemistry 38*, 3478−3490.
20. Schneider, T. R., Gerhardt, E., Lee, M., Liang, P.-H., Anderson, K. S., and Schlichting, I. (1998) *Biochemistry 37*, 5394−5406.
21. Kulik, V., Weyand, M., Seidel, R., Niks, D., Arac, D., Dunn, M. F., and Schlichting, I. (2002) *J. Mol. Biol. 324*, 677−690.
22. Weyand, M., Schlichting, I., Herde, P., Marabotti, A., and Mozzarelli, A. (2002) *J. Biol. Chem. 277*, 10653−10660.
23. Weyand, M., Schlichting, I., Marabotti, A., and Mozzarelli, A. (2002) *J. Biol. Chem. 277*, 10647−10652.
24. Yang, X.-J., and Miles, E. W. (1992) *J. Biol. Chem. 267*, 7520−7528.
25. Yanofsky, C., Ito, J., and Horn, V. (1967) *Cold Spring Harbor Symp. 31*, 151−162.
26. Peracchi, A., Mozzarelli, A., and Rossi, G. L. (1995) *Biochemistry 34*, 9459−9465.
27. Fan, Y. X., McPhie, P., and Miles, E. W. (2000) *J. Biol. Chem. 275*, 20302−20307.
28. Rowlett, R., Yang, L.-H., Ahmed, S. A., McPhie, P., Jhee, K. H., and Miles, E. W (1998) *Biochemistry 37*, 2961−2968.
29. Ahmed, S. A., Ruvinov, S., B., Kayastha, A., M., and Miles, E. W. (1991) *J. Biol. Chem. 266*, 21540−21557.
30. Yang, X.-J., and Miles, E. W. (1993) *J. Biol. Chem. 268*, 22269−22272.
31. Hyde, C. C., Ahmed, S. A., Padlan, E. A., Miles, E. W., and Davies, D. R. (1988) *J. Biol. Chem. 263*, 17857−17871.
32. Sachpatzidis, A., Dealwis, C., Lubetsky, J. B., Liang, P. H., Anderson, K. S., and Lolis, E. (1999) *Biochemistry 38*, 12665−12674.
33. Roy, M., Keblawi, S., and Dunn, M. F. (1988) *Biochemistry 27*, 6698−6704.
34. Kawasaki, H., Bauerle, R., Zon, G., Ahmed, S. A., and Miles, E. W. (1987) *J. Biol. Chem. 262*, 10678−10683.
35. Yang, L.-H., Ahmed, S. A., and Miles, E. W. (1996). *Protein Expression Purif. 8*, 126−136.
36. Yang, L.-H., Ahmed, S. A., Rhee, S., and Miles, E. W. (1997) *J. Biol. Chem. 272*, 7859−7866.
37. Miles, E. W., Kawasaki, H., Ahmed, S. A., Morita, H., Morita, H., and Nagata, S. (1989) *J. Biol. Chem. 264*, 6288−6296.
38. Miles, E. W., Bauerle, R., and Ahmed, S. A. (1987) *Methods Enzymol. 142*, 398−414.
39. Weischett, W. O., and Kirschner, K. (1976) *Eur. J. Biochem. 65*, 365−373.
40. Worthington Enzyme Manual (1993) pp 201−206, New Jersey, Worthington Biochemical Corp.
41. Drewe, W. F., Jr., and Dunn, M. F. (1985) *Biochemistry 24*, 3977−3987.
42. Jhee, K. H., McPhie, P., Ro, H. S., and Miles, E. W. (1998) *Biochemistry 37*, 14591−14604.
43. Ueno, H., Likos, J. J., and Metzler, D. E. (1982) *Biochemistry 21*, 4387−4393.
44. Likos, J. J., Ueno, H., Feldhaus, R. W., and Metzler, D. E. (1982) *Biochemistry 21*, 4377−4386.
45. Fan, Y.-X., McPhie, P., and Miles, E. W. (2000) *Biochemistry 39*, 4692−4703.
46. Houben, K. F., Kadima, W., Roy, M., and Dunn, M. F. (1989) *Biochemistry 28*, 4140−4147.
47. Houben, K. F., and Dunn, M. F. (1990) *Biochemistry 29*, 2421−2429.
48. Harris, R. M., and Dunn, M. F. (2002) *Biochemistry 41*, 9982−9990.
49. Dunn, M. F., Roy, M., Robustell, B., and Aguilar, V. (1987) in *Proceedings of the 1987 International Congress on Chemical and Biological Aspect of Vitamin B6 Catalysis* (Korpela, T., and Christen, P., Eds.) pp 171−181, Birkhauser Verlag, Basel, Switzerland.
50. Drewe, W. F., Jr., and Dunn, M. F. (1986) *Biochemistry 25*, 2494−2501.

BI034291A